Journal of Medicinal Chemistry

pubs.acs.org/jmc

Article

Antibacterial and Anti-Inflammatory Activity of Branched Peptides Derived from Natural Host Defense Sequences

Published as part of Journal of Medicinal Chemistry special issue "Natural Products Driven Medicinal Chemistry".

Giada Meogrossi, Eva Tollapi, Alessandro Rencinai, Jlenia Brunetti, Silvia Scali, Eugenio Paccagnini, Mariangela Gentile, Pietro Lupetti, Simona Pollini, Gian Maria Rossolini, Andrea Bernini, Alessandro Pini, Luisa Bracci, and Chiara Falciani*

Cite This: *J. Med. Chem.* 2024, 67, 16145−16156

Read Online

ACCESS | Metrics & More | Article Recommendations | Supporting Information

ABSTRACT: Antibiotic resistance is a major global health threat, necessitating the development of new treatments and diverse molecules to combat severe infections and preserve the efficacy of existing drugs. Antimicrobial peptides (AMPs) offer a versatile arsenal against bacteria, and peptide structure branching can enhance their resistance to proteases and improve their overall efficacy. A small library of peptides derived from natural host defense peptides and synthesized in a tetrabranched form was selected against *E. coli*. Six selected branched peptides were further studied for antibacterial activity against a panel of strains, biofilm inhibition, protease resistance, and cytotoxicity. Their structure was predicted computationally and their mechanism of action was investigated by electron microscopy and by using fluorescent dyes. The peptide BAMP2 showed promise in a mouse skin infection model, indicating the potential for local infection treatment.

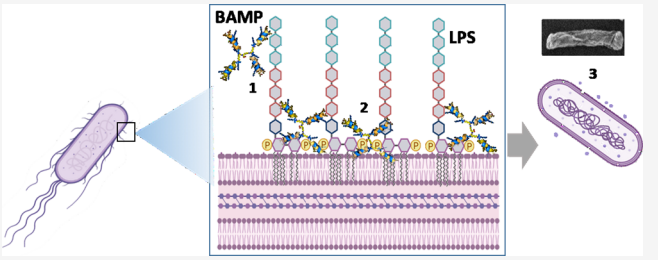

INTRODUCTION

Life-threatening infections due to "superbugs" are becoming more and more frequent, not only in hospitalized and immunocompromised patients but also among young healthy people. The World Health Organization (WHO) warns that antimicrobial resistance (AMR) is an increasingly serious threat to global public health and calls for action across all government sectors and society.[1] Bacteria that cause local and minor infections, for example, of the urinary tract or oral cavity, now show high proportions of resistance in all regions of the world.

Prolonged use of antibiotics contributes to the development and spread of drug-resistant microorganisms. New treatment options are therefore an urgent medical need, and most importantly, every effort must be made to preserve the efficacy of existing antibacterials currently used to treat life-threatening infections. All other uses of new antimicrobials, such as prophylaxis after surgery and treatment of trivial infections, should be addressed with non-life-saving antibiotics. So, not only are new treatment options needed but also different classes of molecules must be administered in the different settings of local and severe infections to preserve life-saving drugs from resistance.

Peptide antibiotics, such as bacitracin, colistin, and daptomycin, are currently employed in managing infectious diseases, while numerous others are undergoing assessment for prospective utilization in the clinics. Natural antimicrobial peptides (AMPs) are found in all classes of living organisms as a part of innate immune responses.[2] They are reported to act as broad-spectrum antibiotics that kill bacteria, viruses, and fungi[3] and also to have immunomodulatory properties.[4] AMPs also showed reduced tendency to promote AMR development in pathogenic bacteria.[5]

AMPs are continuously produced by living organisms due to their short half-life and limited killing power.[2,3] Researchers have experimented with many chemical modifications to overcome their ephemerality. One such modification involves synthesizing the active sequence on a branched core, which provides the entire molecule with an increased half-life and stronger bactericidal activity. Tetrabranched AMPs show promise for fighting multidrug-resistant (MDR) infections due to their broad spectrum of activity and their resistance to proteases and peptidases. As an example, the tetrabranched

Received: April 5, 2024
Revised: August 17, 2024
Accepted: August 22, 2024
Published: September 11, 2024

https://doi.org/10.1021/acs.jmedchem.4c00810
J. Med. Chem. 2024, 67, 16145−16156

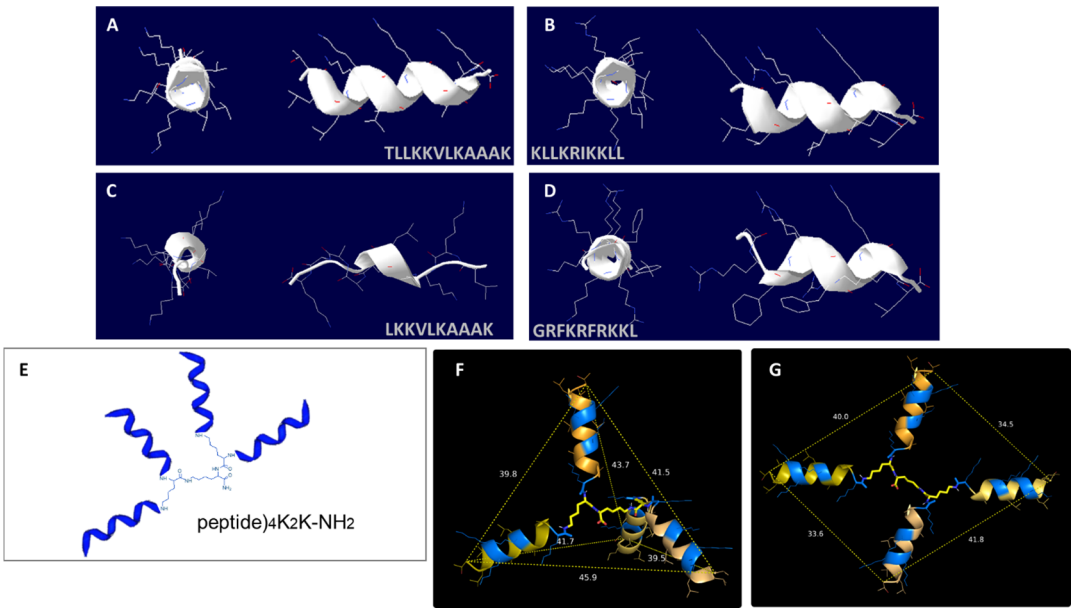

Figure 1. (A–D) Secondary structure calculated for BAMP2, BAMP35, BAMP39, and BAMP49 in a linear form. (E) General structure of BAMPs arranged on a tetrabranched scaffold. (F) Tetrahedral form and (G) the flat square structure of BAMP2. Hydrophilic residues are reported in blue, and hydrophobic residues are reported in yellow.

M33 peptide, a non-natural peptide, with an amphipathic amino acid sequence, very similar to that of natural AMPs, was developed in a preclinical setting. It showed interesting MIC_{90} and biofilm eradication properties against a wide panel of bacterial species. M33 also showed immunomodulatory activity along with in vivo activity in cases of sepsis, pneumonia, and skin bacterial infections in mice.[6−11]

A small library of 18 peptides was obtained using 9−14 residue sequences from natural AMPs. They were synthesized in a tetrabranched form to obtain peptides of particular activity and resistance. A first round of selection against *E. coli* TG1 identified the six most effective sequences that derived from dermaseptin, anoplin, mastoparan, and cathelicidin.

The dermaseptin family of peptides, first isolated from Hylid frogs, are considered promising against Gram-negative and Gram-positive bacteria.[12] There are more than 100 of them, all displaying a typical amphiphilic consensus motif rich in alanine and lysine.

Anoplin was first extracted from the venom of the wasp *Anoplius samariensis* and has shown activity against Gram-negative and Gram-positive bacteria.[13,14]

The mastoparan family is derived from the venom of the wasp *Vespula lewisii* and has strong broad bactericidal activity, accompanied by severe toxicity determined by its hemolytic activity and its triggering of mast cell degranulation.[4]

Cathelicidins are a very large group of AMPs belonging to the innate immunity of most vertebrate species, including mammals, birds, fish, and amphibians. In particular, ChMAP-28 is expressed in leukocytes of the goat *Capra hircus*.[15]

All peptides were synthesized in a tetrabranched form using three lysines as scaffolds to support four equal copies of sequences on the four amino groups of lysines (Figure 1). The underpinning rationale for transforming natural peptides into small dendrimers is related to the possibility of increasing their stability to proteases and binding avidity. Branched peptides display a 10-fold increase in resistance to the proteolytic activity of serum,[16] probably due to their bulkier size that hampers the peptide from fitting into the cleavage site of proteases.[17,18] Multivalency, on the other hand, allows stronger binding to lipopolysaccharide (LPS) and lipoteichoic acid (LTA) of the bacterial outer membrane,[19,20] resulting in quicker killing and favorable immunomodulation.[21] Increased activity and resistance permit lower doses and contribute to overcoming toxicity drawbacks.

The branched peptides were tested for their antibacterial activity, biofilm inhibition, resistance to proteases, and cytotoxicity for eukaryotic cells. Their tertiary structure, particularly their amphipathic arrangement, essential for antimicrobial effectiveness,[11,12] was predicted by a computational protocol. The mechanism of action was investigated by electron microscopy and by using fluorescent dyes to determine membrane integrity. The efficacy of BAMP2 was evaluated in a mouse skin infection model and proved promising for reducing infection and inflammation.

RESULTS

Peptide Synthesis. A small library of 18 peptides was obtained using 9−14 residue sequences from natural AMPs. Sequences were derived from the linear peptides dermaseptin, mastoparan, uperin, defensin, α-chain of bovine hemoglobin (α-CBH), anoplin, and cathelicidin and were selected from the Database of Antimicrobial Activity and Structure of Peptides (DBAASP: https://dbaasp.org/home), filtering them on the basis of their already tested efficacy and low toxicity toward eukaryotic cells, in a linear form.

Branched peptides synthesized via solid-phase synthesis exhibit optimal yields at a length of approximately 15 residues. Longer peptides may tend to aggregate on the resin when their side chains are protected, resulting in poor yields and the formation of numerous byproducts. Ten out of 20 peptides filtered from the database already had an acceptable length, and the others (BAMP37, 39, 41, 44, 45, 46, 49, 52) were divided into two fragments. All of the 18 peptides (Table 1) were synthesized in a tetrabranched form on a multiple automated synthesizer using standard Fmoc chemistry. The

https://doi.org/10.1021/acs.jmedchem.4c00810
J. Med. Chem. 2024, 67, 16145−16156

Table 1. Minimum Inhibitory Concentrations (μM) of the Library against *E. coli* TG1

entry	BAMP	structure	origin	MIC (μM) vs *E. coli* TG1
1	2	TLLKKVLKAAAK)$_4$K$_2$K	dermaseptin	1.5
2	13	INLKAIAALAKKLL)$_4$K$_2$K	mastoparan	12.5
3	18	GIIDIAKKLFESW)$_4$K$_2$K	uperin	12.5
4	21	LSAAHSLAIGRR)$_4$K$_2$K	defensin	25
5	22	LSAARSLAIGRR)$_4$K$_2$K	defensin	12.5
6	23	LRAAHRLAIGRR)$_4$K$_2$K	defensin	12.5
7	26	STVLTSKYR)$_4$K$_2$K	α-CBH	25
8	30	ALLKRIKTLL)$_4$K$_2$K	anoplin	25
9	34	KLLKFIKTLL)$_4$K$_2$K	anoplin	12.5
10	35	KLLKRIKKLL)$_4$K$_2$K	anoplin	6
11	37	KKLLGKNWKLM)$_4$K$_2$K	mastoparan	3
12	39	LKKVLKAAAK)$_4$K$_2$K	dermaseptin	1.5
13	41	LKLKSIVSW)$_4$K$_2$K	mastoparan	12.5
14	44	KRLWHKVGPF)$_4$K$_2$K	cathelicidin	12.5
15	45	INLKKLAKL)$_4$K$_2$K	mastoparan	1.5
16	46	RGLRRLGRKI)$_4$K$_2$K	cathelicidin	12.5
17	49	GRFKRFRKKL)$_4$K$_2$K	cathelicidin	6
18	52	RGLRRLGRKIA)$_4$K$_2$K	cathelicidin	12.5

products were purified and characterized by high-performance liquid chromatography (HPLC) and mass spectrometry (MS) (Figure S1).

Antibacterial Activity. A first round of selection of the 18 peptides was conducted against *E. coli* (Table 1).

The most effective sequences were 12-mer BAMP2, TLLKKVLKAAAK)4K2K, and its 10-mer analogue BAMP39, LKKVLKAAAK)4K2K, dermaseptin derivatives. BAMP35, KLLKRIKKLL)4K2K, is a 10-mer anoplin derivative. The 11-mer BAMP37, KKLLGKNWKLM)4K2K, and the 9-mer BAMP45, INLKKLAKL)4K2K, are mastoparan derivatives. BAMP49, GRFKRFRKKL)4K2K, is a 10-mer derivative reproducing the sequence of ChMAP28, a cathelicidin. This set of 6 peptides was tested in a wide panel of species and strains with different susceptibilities to antibiotics. The MICs of the best BAMPs against Gram-positive and Gram-negative bacteria are presented in Table 2.

The peptides were incubated at 37 °C for 12 h with *E. coli*, *P. aeruginosa*, and *K. pneumoniae* Gram-negative strains and with *E. faecalis*, *E. faecium*, and *S. aureus* Gram-positive strains. All showed a more pronounced effect against Gram-negative species. The activity against *E. coli* TG1, reference strain, ranged from 0.7 to 6 μM. Similarly, against the *E. coli* LC711/14 clinical isolate, the MIC ranged from 3 to 6 μM, except for BAMP37 and BAMP49, which showed lower activity. The *P. aeruginosa* reference strain was susceptible to all peptides in the range 3−6 μM. BAMP2 showed similar activity (12 μM) against the *P. aeruginosa* clinical isolates FI25 and FI29, which carry two different genes conferring β-lactamase resistance. All of the BAMPs showed MICs between 6 and 25 μM against the *K. pneumoniae* reference strain. In the last decade, the emergence of extensively drug-resistant Gram-negative strains has led to the renewed use in the clinical practice of colistin, an AMP; as a result, emergence of resistance due to different acquired mechanisms has been reported. Since colistin and the BAMP peptides are supposed to have a similar mechanism of action, it is of remarkable importance that BAMP2, BAMP35, BAM39, and BAMP45 were active against the colistin-resistant *E. coli* LC711/14, and excluding BAMP39, also against the

Table 2. Minimum Inhibitory Concentrations (μM)

name	BAMP2	BAMP35	BAMP37	BAMP39	BAMP45	BAMP49
sequence	TLLKKVLKAAAK)$_4$K$_2$K	KLLKRIKKLL)$_4$K$_2$K	KKLLGKNWKLM)$_4$K$_2$K	LKKVLKAAAK)$_4$K$_2$K	INLKKLAKL)$_4$K$_2$K	GRFKRFRKKL)$_4$K$_2$K
origin	dermaseptin	anoplin	mastoparan	dermaseptin	mastoparan	cathelicidin
E. coli TG1	1.5	6	3	1.5	0.7	6
E. coli LC711/14	3	6	>25	6	6	>25
P. aeruginosa ATCC 27853	6	6	3	6	3	6
P. aeruginosa FI-25 (bla$_{VIM-1}$[a])	12	NT	NT	NT	NT	NT
P. aeruginosa FI-29 (*bla*$_{GES-5}$[a])	12	NT	NT	NT	NT	NT
K. pneumoniae ATCC43816	6	6	25	12.5	12	25
K. pneumoniae (colR[a])	6	12.5	>25	>25	6	>25
E. faecalis 51299	25	25	>25	>25	>25	>25
E. faecium FI-48 (vanA[a])	6	NT	NT	NT	NT	NT
S. aureus USA300	>25	3	>25	>25	>25	>25

[a]bla$_{VIM-1}$, VIM-1 metallo-β-lactamase; bla$_{GES-5}$, GES-5 β-lactamase; colR, colistin-resistant phenotype; vanA, vancomycin-resistant phenotype; NT, not tested.

https://doi.org/10.1021/acs.jmedchem.4c00810
J. Med. Chem. 2024, 67, 16145−16156

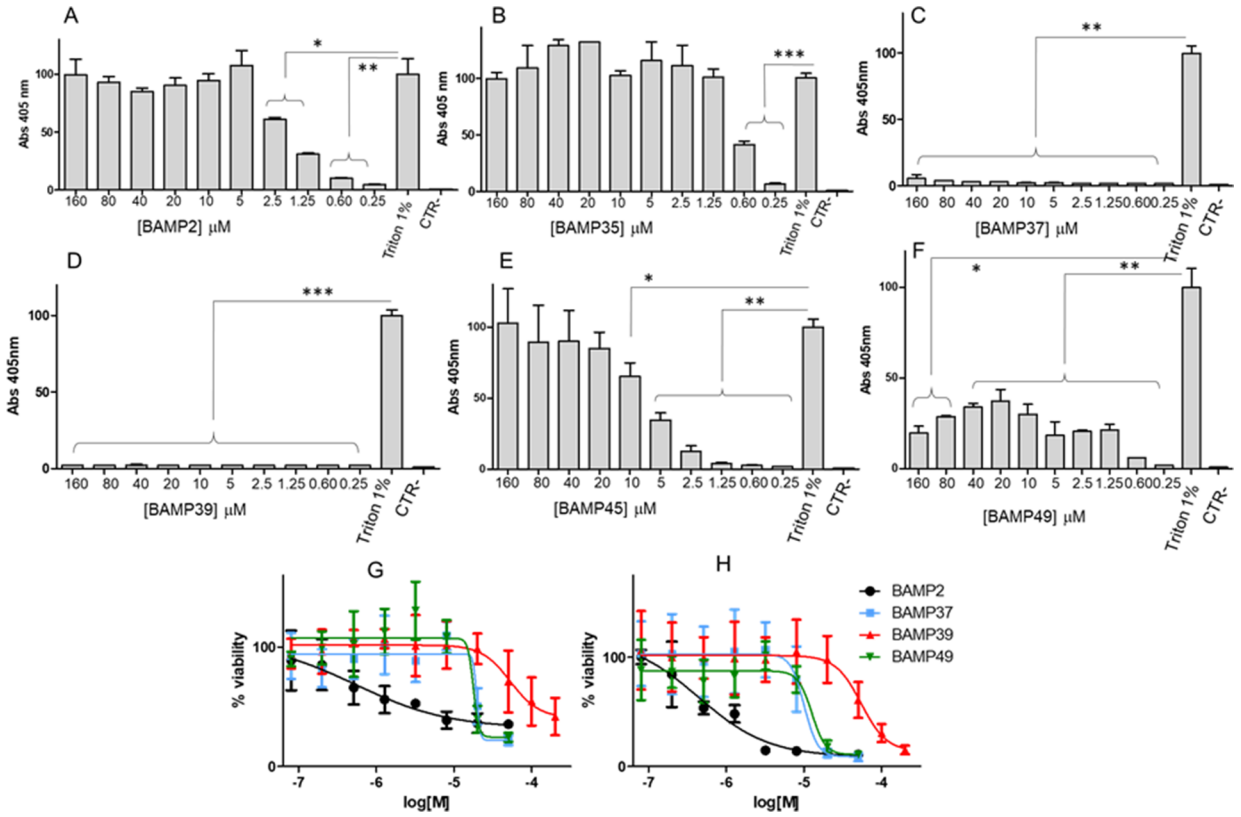

Figure 2. (A–F) Hemolytic activity of BAMP peptides at 37 °C for 2 h. All experiments were repeated at least three times (n = 3), statistical analysis was performed using the paired two-tailed t test. The asterisk indicates significant differences between columns (*p < 0.05; **p < 0.01; ***p < 0.001). (G) 4 h and (H) 24 h cytotoxicity of the peptides against RAW264.7 murine macrophages.

colistin-resistant *K. pneumoniae* colR strain. Activity against *E. faecalis* and *S. aureus* Gram-positive strains was poor for all peptides, except from BAMP35 toward *S. aureus* USA300 that showed an MIC of 3 μM and BAMP2 against *E. faecium* FI-48 with an MIC of 6 μM. Monomeric analogues (MONO2, MONO35, MONO37, MONO39, MONO45, and MONO49) of the six selected lead sequences were synthesized in a linear form and tested against *E. coli* TG-1 to confirm the gain in efficacy of the branching strategy. In fact, for all six peptides, the MIC was higher than the maximum tested concentration, 25 μM (Table S1).

Tertiary Structure Prediction. The peptide sequences were analyzed with the APPTEST protocol,[22] which produces a pdb file reproducing the image of the tertiary structure of the linear analogue. The application calculates the 3D structure of linear sequences in water.

BAMP2 and BAMP35 displayed an amphipathic α-helix involving all residues except the first and last (Figure 1A,B). BAMP39, a short analogue of BAMP2, showed an α-helix that involved only the three central residues (VLK) (Figure 1C). The cathelicidin derivative BAMP49 was fully arranged in an amphipathic α-helix (Figure 1D), whereas the mastoparan derivatives BAMP37 and BAMP45 showed a random linear arrangement. Since the amphipathic nature of AMPs is essential for their antimicrobial effectiveness and selectivity,[11,12] we accommodated the four arms on a tetrabranching core to confirm that the predicted structures were maintained in the tetrabranched form. Two forms were analyzed: the tetrahedral form, in which the four branches were at a maximum distance pointing the vertices of a tetrahedral pyramid (Figure 1F), and the flat square structure, where the four arms were on the same plane (Figure 1G); BAMP2 is reported in both forms as an example. The tetrahedral form spontaneously occurred when all peptide bonds were in trans, and the phi and psi angles aligned with the Ramachandran plot, being energetically favored. This configuration remains stable in a flat square form. The transition from the tetrahedron to flat square form occurred with minimal torsion of the central lysine side chain, without disruption of the peptide bonds and their associated phi and psi angles. Notably, in the flat square form, all four lysines of the active sequence are exposed on the same side, while the hydrophobic residues are exposed on the opposite side. Besides, the tetrabranching core itself exposes carbonyl groups and the central side chains on the hydrophobic side, while the HN groups are on the opposite side. The whole structure thus showed an amphipathic structure.

Cytotoxicity of Branched Antimicrobial Peptides. Red blood cell toxicity is a common concern with AMPs, often attributed to the slightly negative charge of erythrocytes. This characteristic makes them susceptible to the cytotoxic effects of cationic AMPs. To assess hemolysis, we conducted a standard colorimetric test, measuring the absorption (405 nm) of hemoglobin after a 2 h incubation at 37 °C with various peptide concentrations.

BAMP2 exhibited hemolysis at 5 μM, while its shorter analogue, BAMP39, showed no hemolytic activity even at concentrations 10 times the minimum inhibitory concentration (MIC). BAMP35 displayed hemolysis at 1.25 μM, indicating higher toxicity at lower concentrations. BAMP45 and BAMP49 induced hemolysis around 15 μM. In contrast, the mastoparan

https://doi.org/10.1021/acs.jmedchem.4c00810
J. Med. Chem. 2024, 67, 16145–16156

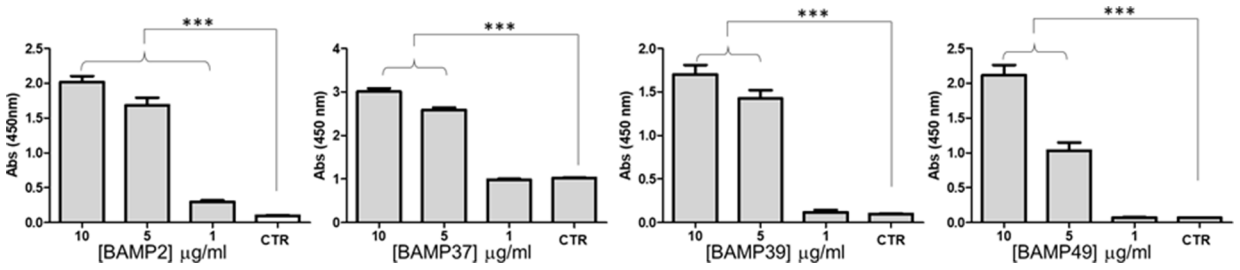

Figure 3. Binding of BAMPs to LPS was tested by ELISA with LPS−biotin and streptavidin−POD. ***$p < 0.0001$, $n = 12$.

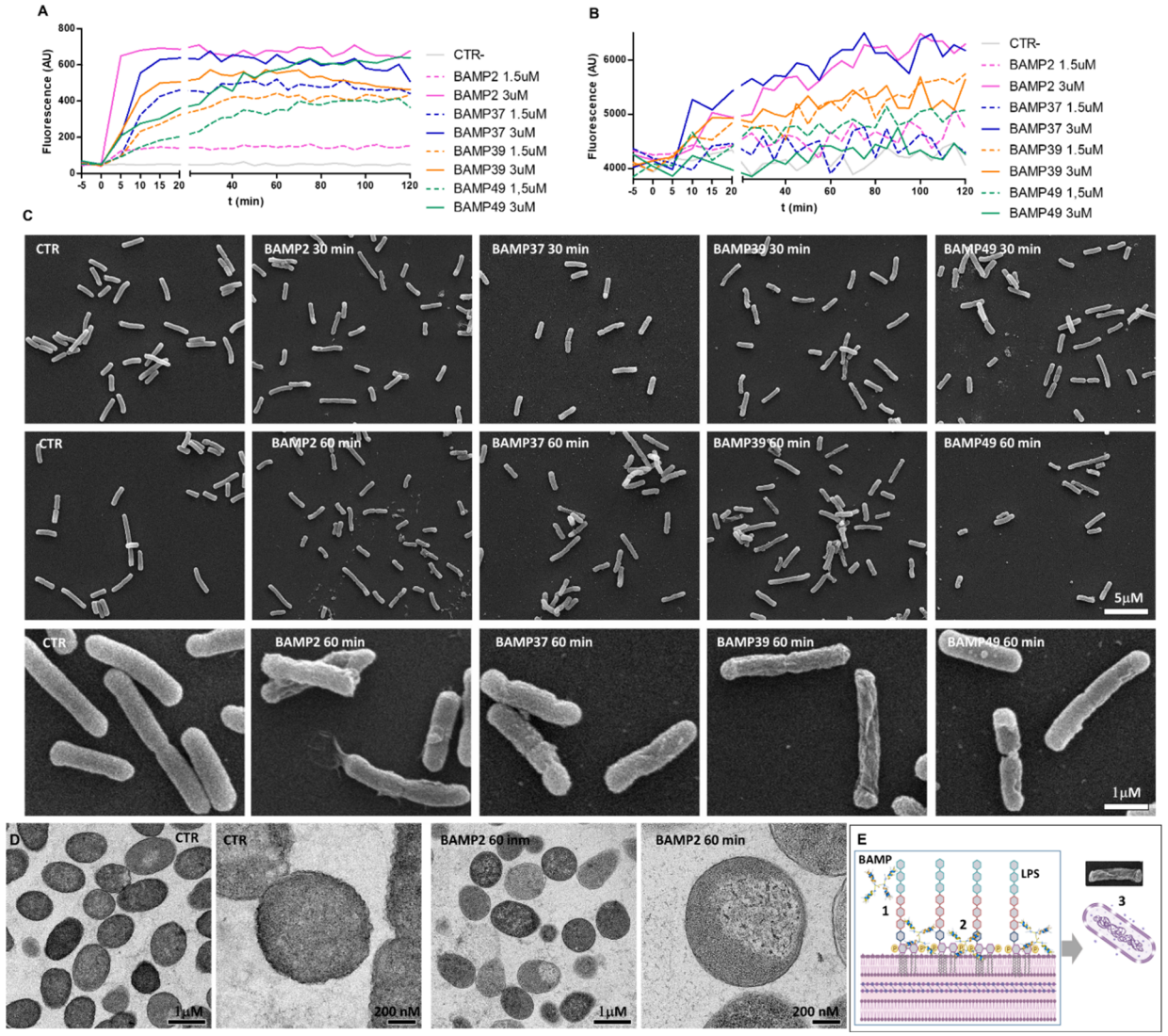

Figure 4. (A,B) Cytoplasmic membrane permeability of *E. coli* on treatment with the BAMPs at the MIC and twice the MIC. Fluorescence due to binding of PI (A) and Sytox green (B) fluorescent probes with DNA was measured at 535−617 and 480−523 nm excitation and emission wavelengths, respectively, with a plate reader. The data is expressed as means (±SD) of three independent repeats in triplicate. (C) SEM images of *E. coli* treated with the peptides for 30 and 60 min and (D) TEM images of *E. coli* treated with the peptide BAMP2, where the loss of outer membrane double layer and blisters are visible. (E) Model of the BAMPs 3-step mechanism of action: 1—electrostatic interaction of positive charges on the peptide and LPS, 2—embedding into the membrane, thanks to amphipathic helix structure, and 3—loss of membrane functionality (created with BioRender.com).

derivative BAMP37 demonstrated no hemolytic activity (Figure 2A−F).

RAW264.7 murine macrophages were used to test the toxicity in a eukaryotic model. Cell viability was measured in a colorimetric assay after 4 and 24 h of incubation, respectively (Figure 2G,H), with peptides at different concentrations. The slopes were similar for both time points, but 100% cell killing was only observed at 24 h. Among the peptides tested, BAMP39 exhibited the least toxicity, requiring a concentration of 200 μM to achieve 100% cell killing, with an LC50 of 5.455e−005 M. In contrast, the other peptides, BAMP2, BAMP37, and BAMP49, demonstrated higher toxicity with

https://doi.org/10.1021/acs.jmedchem.4c00810
J. Med. Chem. 2024, 67, 16145−16156

LC50 values of 4.405e−007, 1.000e−005, and 1.258e−005 M, respectively. In fact, BAMP2, BAMP37, and BAMP49 induced complete cell death at concentrations 1 log lower than that required for BAMP39 (Figure 2G,H).

Mechanism of Action. *BAMP Binding to LPS.* AMPs belong to a large family of molecules that share an analogue mechanism of action against bacteria. Like many other AMPs of natural origin, BAMPs are rich in cationic amino acid residues with a net positive charge that draws them to negatively charged components, such as LPS and LTA, on the bacterial surface. Typically, the inner core of LPS contains a few molecules of KDO (3-deoxy-α-D-manno-octulosonic acid), a negatively charged portion of the macromolecule located very close to the bacterial membrane. The electrostatic interaction between LPS and the peptides accounts for part of the selectivity of AMPs for bacteria rather than eukaryotic cells and is therefore very important. Also, the ability to bind LPS proves crucial in stemming the onset of inflammation; in this sense, AMP proved to be able to neutralize LPS and prevent the severely toxic effects of LPS, mainly released during sepsis.

All peptides bound to LPS in a dose-dependent manner (Figure 3). ELISA was run using LPS−biotin and streptavidin−peroxidase (POD) on the peptides adsorbed in wells.

Interaction with Bacterial Outer Membranes. After the first step of the killing machinery, which is the interaction of the peptides with LPS or LTA, the peptides act mainly by interacting with bacterial membranes and impairing their function and general homeostasis, leading to cell distress and eventually death. Similarities in the killing mechanisms of AMPs are due to typical features of their structure, such as amphipathicity and charge.[23−25]

The membrane damaging effect of these peptides against *E. coli* TG1 was assessed using two fluorophores, PI and Sytox green.[26,27] The two dyes are actively fluorescent when they bind to nucleic acids, which happens only when the cytoplasmic membrane is critically damaged. The effect of the peptides in increasing membrane permeability was already visible after 10 min of incubation for all peptides at twice the MIC. Dose dependency was also appreciable for all BAMPs. The increase in fluorescence of the two fluorescent dyes reached a plateau after only 10 min at the higher concentrations and after 40−50 min when the peptides were used at exactly the MIC (Figure 4A,B). Electron microscopy was also used to qualitatively describe the membrane effect of the peptides on *E. coli*. Scanning electron microscopy (SEM) micrographs taken after 30 or 60 min incubations with twice the MIC showed deterioration of the membrane, wrinkling of the surface, enlargement of bacterial cells, and overall loss of surface smoothness, as evident in the untreated control bacteria (Figure 4C). The qualitative effect was similar at the two time points, but the frequency was higher with longer incubation.

Transmission electron microscopy (TEM) was conducted on *E. coli* for the 60 min treatment with the BAMP2 peptide, taken as an arbitrary model for all peptides, and showed the loss of outer membrane double layer integrity and formation of blisters on the outside of the cell (Figure 4D). The mechanism of action of BAMPs can be then described in three main steps: (1) interaction with LPS: BAMPs bind LPS with multivalent interactions that create a much stronger binding than the sum of the corresponding monovalent interactions achieved with monomers;[19,20] (2) thanks to their amphipathic structure, BAMPs embed themselves into the membrane using the hydrophobic face at first;[11,12] and (3) the embedding of BAMPs leads to the disruption of the membrane integrity, compromising its functionality and eventually viability of the cells (Figure 4E).

Stability to Serum Proteolysis. In clinical practice, the main hurdle in the development of peptides as antibiotics is their short half-life. Peptides are quickly degraded by proteases and peptidases, indeed the endogenic peptides of the innate immunity of organisms have to be produced continuously by cells.[28] Tetrabranched peptides are known to have an increased resistance to proteases compared to their linear analogues because their branching scaffold hinders access to proteolytic enzyme-binding sites.[18] We tested the stability of the BAMP peptides in serum, employed as a model of a complex mixture of proteases.

Tetrabranched peptides BAMP2, BAMP37, BAMP39, and BAMP49 and their linear analogues MONO2, MONO37, MONO39, and MONO49 were incubated for 4 and 24 h at 37 °C. HPLC analysis, followed by MS, confirmed the presence or absence of the intact peptide (Table 3 and Figures S2−S4).

Table 3. Serum Stability of the Peptides after 4 and 24 h of Incubation at 37 °C[a]

name	sequence	peak presence after 4 h	peak presence after 24 h
BAMP2	TLLKKVLKAAAK)$_4$K$_2$K	yes	yes
MONO2	TLLKKVLKAAAK	yes	no
BAMP37	KKLLGKNWKLM)$_4$K$_2$K	yes	yes
MONO37	KKLLGKNWKLM	no	no
BAMP39	LKKVLKAAAK)$_4$K$_2$K	yes	yes
MONO39	LKKVLKAAAK	no	no
BAMP49	GRFKRFRKKL)$_4$K$_2$K	yes	no
MONO-49	GRFKRFRKKL	yes	no

[a]Branched peptides are compared with their linear analogues.

HPLC and MS graphs showed degradation for all peptides though the peaks of all of the branched peptides, except BAMP49, were still observable and intact after 24 h of incubation. All monomeric analogues were completely degraded in 24 h; MONO37 and MONO39 were already hydrolyzed at 4 h (Table 3). We also observed around 5−10% oxidation of methionine of BAMP37 by MS.

Biofilm Inhibition Activity. Biofilm matrix disruption is crucial for eradicating bacteria since it exposes them to treatments. AMPs are known for their ability to penetrate dense protective bacterial biofilms, presumably by virtue of their amphipathic surfactant nature.[29]

Biofilm inhibition activity was evaluated on the basis of two parameters: the biofilm prevention concentration (BPC) and minimal biofilm inhibition concentration (MBIC).[30] The BPC is the lowest concentration of peptide that results in 20% biofilm formation with respect to untreated controls. The biofilm was measured after removing planktonic cells by washing the wells, which were previously incubated for 24 h with the bacteria and the peptide. MBIC is the lowest concentration of peptide that results in an 80% reduction in the preformed biofilm with respect to untreated controls. A 24 h biofilm was challenged with serial dilutions of the peptides for 14 h. The residual biofilm was measured after removal of planktonic cells. The 96-well plates with peg lids were employed, and absorbance at 595 nm was used to measure the biofilm in both cases.

https://doi.org/10.1021/acs.jmedchem.4c00810
J. Med. Chem. 2024, 67, 16145−16156

Table 4. Biofilm Inhibitory Concentrations (μM)[a]

	E. coli TG1				*K. pneumoniae* ATCC 43816			
μM	BAMP2	BAMP37	BAMP39	BAMP49	BAMP2	BAMP37	BAMP39	BAMP49
MIC	1.5	3	1.5	6	6	25	12.5	>25
BPC	1.5	3	6	25	50	50	>50	50
MBIC	3	25	50	50	50	50	50	50

[a]BPC, biofilm prevention concentration; MBIC, minimal biofilm inhibition concentration.

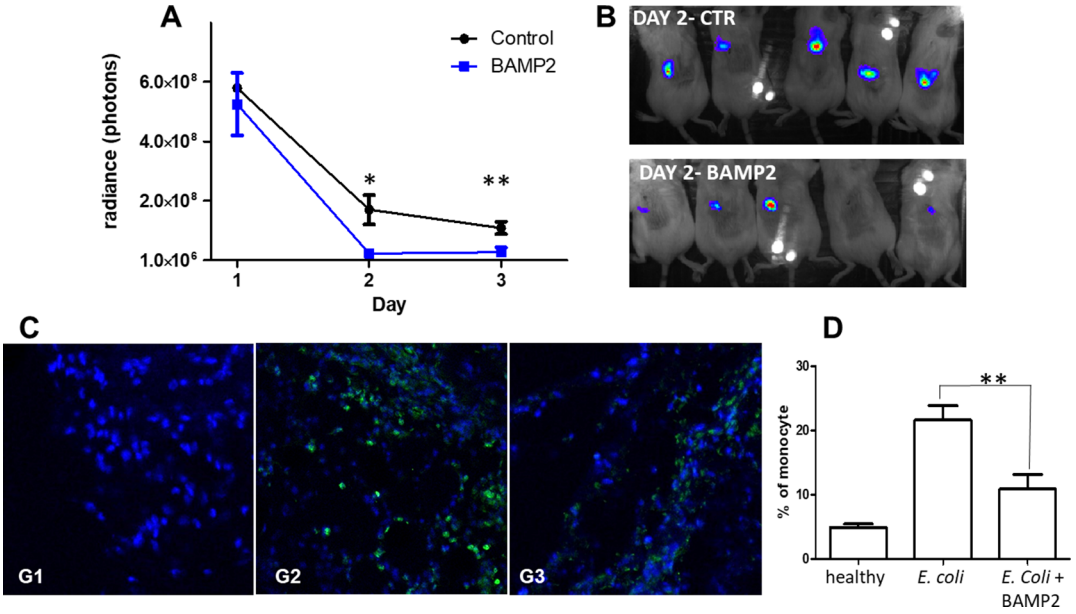

Figure 5. Model of an *E. coli*-luxCDABE skin infection. (A) The number of *E. coli* cells was measured in radiance with an IVIS Lumina X5 imager. The two groups, treated with BAMP2 and untreated, were compared. The unpaired *t* test was run with $n = 5$, 95% confidence interval, $p < 0.05$. (B) Images taken 48 h after infection of the group treated with BAMP2 and of the untreated control group (white dots are an artifact of the visible light beam used to take the picture, not calculated in radiance). (C) Immunohistochemistry of fixed cryosections of skin. The blue signal (DAPI) was used to evaluate the total number of cells in the tissue slice sample, and the green signal (anti-Ly6-G/Ly6-C-488) indicates monocytes. (D) Percentage of monocytes on the total number of cells. Confocal microscopy images were analyzed with ImageJ ($n = 3-6$), followed by the two-tailed *t* test (**$p < 0.05$).

In *E. coli*, BAMP2 and BAMP37 showed a BPC equal to the MIC; BAMP2 was also efficient in removing the preformed biofilm at a concentration double the MIC (Table 4). For BAMP37, the MBIC was eight times the MIC. BAMP39 and BAMP49 showed a BPC four times the MIC. The MBIC of BAMP39 and BAM49 was weaker (50 μM). The *K. pneumoniae* biofilm was more resistant to treatment with all BAMPs (Table 4).

Efficacy of BAMP2 in Skin Infections. Animals were infected with 1×10^8 CFU *E. coli*-luxCDABE subcutaneously on the back and treated locally by sc injection for three consecutive days with BAMP2 (16 mg/kg). *E. coli*-luxCDABE was obtained by transfection of *E. coli* TG1 with the pGEN-luxCDABE plasmid, as kindly donated by Harry Mobley (Addgene plasmid # 44918; http://n2t.net/addgene:44918; RRID:Addgene_44918). All bacteria were grown at 35 °C and 90% humidity in their specific medium.[31]

Images of the mice's backs were taken every day and recorded as radiance. The group treated with BAMP2 showed a 75% reduction in bacterial burden compared to the untreated group on day 2 when the maximum difference was appreciable (Figure 5A). Differences between the treated and untreated group were calculated on the media radiance of each group, at each time point, and proved significant on days 2 and 3. The luminescence was attenuated over time in all groups as an effect of the immune response of the mice and the decay of luciferase expression.

AMPs are also known to have immunomodulatory properties that contribute to the resolution of inflammation, preventing excessive prolonged inflammatory responses that can lead to tissue damage or shock, as in sepsis. AMPs modulate immune response by binding LPSs and LTA and modulating cytokine production.[32] Anti-inflammatory properties of BAMP2 were tested in the in vivo model by measuring inflammatory monocyte recruitment at the site of infection, using a specific antibody (anti-Ly6-G/Ly6-C) on harvested tissue slices.[33] Healthy skin from uninfected animals showed an extremely low presence of monocytes, whereas recruited immune cells were more than 20% higher in infected skin (Figure 5C,D). In treated mice, the monocyte number was almost reduced to that of heathy skin, showing that BAMP2 could significantly impair inflammation.

DISCUSSION AND CONCLUSIONS

AMPs represent an endless resource against bacteria. The sequences almost always need to be adjusted to address their possible use as drugs. Branching of the sequence is an easy and successful way to improve protease resistance and efficacy.[15]

Multivalency, in fact, allows for stronger binding to LPS and LTA compared to single sequences,[19,20] resulting in quicker

https://doi.org/10.1021/acs.jmedchem.4c00810
J. Med. Chem. 2024, 67, 16145−16156

killing and also favorable immunomodulation. Here, we demonstrated that BAMP2, BAMP35, BAMP37, BAMP39, BAMP45, and BAMP49 were active against planktonic forms of Gram-negative strains of *E. coli*, *P. aeruginosa*, and *K. pneumoniae*. Notably, BAMP2, BAMP35, BAM39, and BAMP45 were also active against strains with a resistant phenotype toward colistin, a peptide antibiotic used in clinical practice. The monomeric analogues MONO2, MONO 35, MONO 37, MONO 39, MONO 45, and MONO 49, screened in a microdilution test against *E. coli* TG-1, were discarded from further testing because they were not active at the maximum concentration tested (25 μM). The activity of the peptides then proved to be correlated with their branched structure and also to their tertiary structure. Specifically, BAMP2 showed the most extensive α-helix arrangement and the highest activity. The superior efficacy of BAMP2 was also coupled with a stronger hemolytic effect that will prevent intravenous administration of the drug. The peptides acted by disrupting the bacterial membrane, which manifested as wrinkling of the surface, enlargement of the cells, and an overall loss of surface smoothness. The loss of membrane integrity allowed the internalization of nonpermeable dyes in as little as 10 min after adding the peptides, demonstrating rapid dysregulation of homeostasis. Protease resistance was ensured by the branched structure and proved effective in increasing the peptide half-life in serum. Like many other AMPs of natural origin, BAMPs have a cationic structure that binds LPS in a dose-dependent manner at concentrations around the MIC or half the MIC, 10 and 5 μg/mL, respectively. The ability to bind LPS is a prerequisite for the anti-inflammatory activity shown by many AMPs. Biofilm is a dense complex matrix that protects bacteria against desiccation and leaching. As a barrier to antibiotics, it is the cause of persistent infections. AMPs have an amphipathic surfactant structure that facilitates penetration of the matrix down to the outer bacterial membrane. BAMP2 proved the best against the *E. coli* biofilm, inhibiting its formation and disrupting the existing layers at the MIC and double the MIC, respectively. BAMP37, BAMP39, and BAMP49 were more efficient at inhibiting biofilm formation and less efficient at disrupting the existing *E. coli* biofilm. The *K. pneumoniae* biofilm was 80% disrupted by higher concentrations, i.e., 50 μM, by all peptides.

Based on its superior MIC and antibiofilm activity, BAMP2 was chosen for evaluation in a mouse skin infection model. In vitro results as a whole supported the selection of BAMP2 for in vivo testing. Notably, BAMP2 showed significant efficacy in reducing bacterial load within 48 h, combined with a marked decrease in local recruitment of immune cells at the site of infection. The observed effects are presumably due to the peptide's capacity to lower bacterial burden, and the direct impact thereof, in treated animals. BAMP2's high affinity for LPS suggests that the peptide may mask toxins and impede chemotaxis, contributing to the overall reduction in immune cell recruitment.

The escalating threat of AMR, which poses severe health risks, emphasizes the immediate need to boost the production of new antibiotics and explore innovative strategies in the fight against infectious diseases. In this study, natural AMPs with sequences optimized by branching proved optimal profiles of protease resistance and efficacy. BAMP2, BAMP35, BAMP37, BAM39, BAMP45, and BAMP49 proved to be effective against Gram-negative strains, including colistin-resistant strains. BAMP2, with a superior α-helix arrangement, demonstrated the highest activity. The branched peptides disrupted bacterial membranes, causing structural changes and a rapid dysregulation of homeostasis. Protease resistance, attributed to the branched structure, increased the peptide half-life in serum. The cationic structure of BAMPs facilitated binding to LPS, which is made stronger by multivalency, and was also crucial for their anti-inflammatory activity. Notably, BAMP2 exhibited significant efficacy against the *E. coli* biofilm, inhibiting the formation and disrupting the existing layers. In a mouse skin infection model, BAMP2 demonstrated notable efficacy in reducing the bacterial load and decreasing local immune cell recruitment, likely attributed to its impact on bacterial burden and high LPS affinity.

The characteristics of BAMPs hold significance for the development of novel antimicrobial agents, particularly those against MDR strains. The cost effectiveness and minimal environmental impact of these natural molecules are poised to incentivize investments in new antibiotic options, which have been overlooked by the pharmaceutical industry since the 80s−90s. Besides, the development of a new class of antibiotics, to be used for non-life-threatening infections, would preserve efficacy to the already available antibiotics from further development of resistances, while offering an efficient treatment option for prophylaxis and for minor infections.

EXPERIMENTAL SECTION

Peptide Synthesis. All of the peptides were solid-phase synthesized on a Syro multiple peptide automated synthesizer (MultiSynTech, Witten, Germany) using standard Fmoc chemistry. The resin used was a TentaGel-PHB 4 branch β Ala Wang-type resin (Rapp Polymere, Germany), which is functionalized with the branching lysine core in L-form, $Fmoc_4$—Lys_2—Lys—β-Ala, as previously described. The linear homologues (MONO2, MONO35, MONO37, MONO39, MONO45, and MONO49) were synthesized on a TentaGel-PHB Wang-type resin (Rapp Polymere, Germany) by the same procedure. Side-chain-protecting groups were 2,2,4,6,7-pentamethyldihydrobenzofuran-5-sulfonyl for R, t-butoxycarbonyl for K, and t-butyl for S. The final product was cleaved from the solid support, deprotected by treatment with TFA containing triisopropylsilane and water (95/2.5/2.5), and precipitated with diethyl ether. Crude peptide was purified by reversed-phase chromatography on a Phenomenex Jupiter C18 column (300 Å, 10 mm, 250, 610 mm), using 0.1% TFA/water as eluent A and methanol as eluent B, in a linear gradient from 80% A to 20% A in 30 min. Final peptide purity and identity were confirmed by reversed-phase chromatography on a Phenomenex Jupiter C18 analytical column (300 Å, 5 mm). All compounds were >95% pure by HPLC analysis, as reported in Figure S1.

Bacterial Strains. *E. coli* TG1, *P. aeruginosa* ATCC 27853, *K. pneumoniae* ATCC 43816, and *E. faecalis* ATCC 51299 were the reference strains susceptible to all standard antibiotics. *S. aureus* USA300 was used as a methicillin-resistant reference strain. *E. coli* LC711/14, *K. pneumoniae* colR, *P. aeruginosa* FI-25, *P. aeruginosa* FI-29, and *E. faecium* FI-48 were clinical isolates provided by the Careggi University Hospital. *E. coli*-luxCDABE was obtained by transfection of *E. coli* TG1 with the pGEN-luxCDABE plasmid, kindly provided as a gift from Harry Mobley (Addgene plasmid # 44918; http://n2t.net/addgene:44918; RRID:Addgene_44918). All bacteria were grown at 35 °C and 90% humidity in their specific medium.

Minimum Inhibitory Concentrations. MICs of BAMP2, BAMP39, BAMP37, BAMP45, and BAMP49 and monomeric analogues MONO2, MONO39, MONO37, MONO45, and MONO49 were determined in triplicate against a panel of reference and clinical strains using a microdilution assay. Briefly, a single colony of each strain was grown in its own proper medium at 37 °C. Then, the overnight preculture was diluted 1:100 in cation-adjusted Mueller Hinton Broth (Sigma-Aldrich) and grown at 37 °C up to an optical

https://doi.org/10.1021/acs.jmedchem.4c00810
J. Med. Chem. 2024, 67, 16145−16156

density (OD) of 0.15, measured with a densitometer at 600 nm (Densichek, bioMèrieux, Marcy l'Etoile, France). Wells of a microtiter plate containing 50 μL of serial-doubling dilutions of the peptides were inoculated with an equal volume of 1:100 diluted bacterial suspensions. The final bacterial inoculum was 5×10^4 CFU/well in a volume of 100 μL. The microtiter plate was then incubated at 35 °C for 18−20 h, and MICs were measured either by turbidometry or by visual inspection. Assays were performed in triplicate, and the median MIC values were recorded.

Peptide Structure Modeling. Prediction of BAMP2, BAMP39, BAMP37, BAMP45, and BAMP49 tertiary structures was obtained by APPTEST, a novel computational protocol that employs neural network predictive power and structural biology software programs XPLOR-NIH and CYANA. The neural networks of APPTEST were constructed using experimental model structures acquired from the Protein Data Bank [PDB, https://www.rcsb.org/, accessed on 23 March 2023] to predict structural constraints, which are used in restrained molecular dynamic simulations to produce a final set of structures. The three-lysine scaffold was modeled using CHARMM-GUI[34] and modified residues herein, while four copies of each peptide were merged with the scaffold via the peptide bond with PyMol (PyMOL Molecular Graphics System, Version 2.5. Schrodinger, LLC, 2023). PyMol was also used for structural representation and analysis.

Hemolytic Activity. Whole human blood in EDTA was centrifuged at 3500 rpm for 10 min. The pellet of red blood cells was resuspended at a 1:50 ratio in 1× PBS, mixed by inversion, and incubated with serial dilutions of the peptides from 0.3 to 160 μM in PBS for 2 h at 37 °C. Finally, the plate was centrifuged at 1200 rpm for 5 min. The supernatants were transferred to a 96-well F-plate, and absorbance was measured at 405 nm by using a plate reader. Data for 100% hemolysis was obtained by adding 1% Triton X-100 in PBS to the cells. PBS was used as a negative control. The hemolysis rates of the peptides were calculated with the following equation: Hemolysis (%) = (A peptide − A physiological solution)/(A triton − A physiological solution) 100%, where A is the absorbance.

Eukaryotic Cell Viability Assay. RAW264.7 murine macrophages were seeded in 96-well flat bottom plates at a concentration of 5×10^4 cells/well in 200 μL/well culture medium, Dulbecco's Modified Eagle's Medium (DMEM). The plate was incubated for 24 h at 37 °C in a 5% CO_2 atmosphere. Following incubation, the supernatant was removed and 200 μL of peptides at different concentrations in fresh medium was added to the wells. The plate was then incubated at 37 °C for 4 and 24 h.

After incubation, the wells were washed three times with sterile PBS and fixed with 200 μL of 4% PFA in PBS for 15 min at room temperature. Wells were then washed three times with water, and crystal violet (1% in water) was added and incubated for 30 min in the dark. Finally, wells were washed again and incubated with ethanol/acetone (80:20) to dissolve the color, which was read at 595 nm.

Bacterial Membrane Interaction. A single colony of *E. coli* TG1 was grown in 2xTY medium at 37 °C. The overnight preculture was diluted 1:100 in its own medium and grown at 37 °C up to an OD of 0.2, measured with a densitometer (Densichek, bioMèrieux, Marcy l'Etoile, France), and then centrifuged at 4000 rpm for 10 min. The resulting bacterial pellet was resuspended in PBS-glucose and incubated with 5 μg/mL propidium iodide (PI) or SYTOx Green concentrated to 5 μM. The suspension was vortexed, and 100 μL was added to the wells of a black 96-well plate (Optiplate). The samples were preincubated at 37 °C for 15 min, and then the fluorescence was measured every 30 s for 5 min with a plate reader (Victor Nivo, PerkinElmer) to stabilize the fluorophore signal. The plate was then ejected, and peptides concentrated to 1.5 and 3 μM were added in duplicate wells. The plate was immediately returned to the reader to continue measuring PI and SYTOx green fluorescence every minute for 100−120 min (PI; λ_{ex} = 535 nm, λ_{em} = 617 nm; SYTOx green λ_{ex} = 504 nm, λ_{em} = 523 nm).

Scanning Electron Microscopy. A single colony of each bacterium was grown in its medium overnight at 37 °C. The overnight preculture was diluted at a 1:100 ratio in bacterial broth and measured with a densitometer (Densichek, bioMèrieux, Marcy l'Etoile, France) until reaching OD = 1. Then, 4 mL of this bacterial suspension was distributed in Falcon tubes and centrifuged for 10 min at 4000 rpm. The supernatant was discarded, and the pellet was resuspended in 2 mL of 1× PBS containing peptides and incubated for 30 min and 1 h. The final concentration of the peptides was 12 μM. Untreated bacteria were used as positive controls.

Each sample was transferred to a 2 mL Eppendorf tube, centrifuged at 10000 rpm for 5 min, and the pellet was resuspended in 500 μL of sterile 1× PBS. In the meantime, glass coverslips were placed at the bottom of a 24-well plate, and 20 μL of the samples was dropped onto each. After 5 min, the excess was removed and washed with 20 μL of 0.1 M cacodylate buffer (CB). The cells were then fixed in 2.5% glutaraldehyde in CB for 2 h at 4 °C, washed in CB, postfixed with 1% osmium tetroxide in water for 1 h at 4 °C, and dehydrated in an ascending alcohol series. Ethanol was then replaced with tert-butanol, and the samples were frozen and dried by sublimation. The coverslips were mounted on specimen stubs and coated with 20 nm gold/palladium (60/40) using a Balzers MED010 sputter coater. Sample survey and imaging were performed with an FEI Quanta400 scanning electron microscope operating at an electron acceleration voltage of 20 kV.

Transmission Electron Microscopy. Bacteria were grown and incubated with peptides, as described above, for SEM sample preparation. Each sample was transferred to a 2 mL Eppendorf tube. The tubes were then centrifuged at 10,000 rpm for 5 min. The cell pellets were fixed in 2.5% glutaraldehyde in CB for 2 h at 4 °C, washed in CB, and postfixed with 1% osmium tetroxide in water for 1 h at 4 °C; they were dehydrated in an ascending alcohol series, incubated twice in propylene oxide, infiltrated and embedded in Epon resin (Glycid ether 100, Serva Electrophoresis), and then polymerized in an oven at 60 °C for 48 h.

Ultrathin sections (65 nm) of the sample were obtained with a Reichert-Jung ultracut E ultramicrotome and collected on 150 mesh copper grids. Section staining was performed with uranyl acetate and a lead citrate solution. Stained sections were imaged by a transmission electron microscope (FEI Technai G2 SPIRIT, acceleration voltage 100 kV), equipped with a TemCam F216 Tvips CMOS camera.

Stability to Serum Proteolysis. A pool of sera from healthy volunteers (n = 4) was diluted 25% using RPMI 1640 medium. Each peptide at a concentration of 180 μM was incubated in the diluted serum at 37 °C for 4 and 24 h. After the established time, the sample was added to trichloroacetic acid, diluted 15% in water, held at 4 °C for 5 min, and then centrifuged at 12,000−13,000 × g for 5 min. The resulting supernatant was diluted with 0.1% TFA/water (750 μL) and used for HPLC analysis (250 μL). The sample containing the peptide peak collected by HPLC (2 μL) was used for MALDI-TOF analysis. Time-zero HPLC and MS-spectroscopy spectra were obtained immediately after mixing each peptide with 25% serum. The presence of the intact peptide was established by HPLC by spotting and integrating the peptide peak at the correct retention time. Then, MALDI-MS was performed to confirm the identity of the peptide peak.

Binding to LPS. BAMP2, BAMP39, BAMP37, BAMP45, and BAMP49 were diluted in carbonate buffer (pH 9) and used at working concentrations of 10 μg/mL, 5 μg/mL, and 1 μg/mL to coat a 96-well ELISA strip plate. Uncoated wells were used as negative controls. The plate was then sealed and incubated overnight at 4 °C. After the well contents were aspirated, the plate was washed three times with PBS + 0.05% Tween 20 and then three times with only PBS for removing residues of detergents. Saturation of the plate was performed by adding 400 μL/well of 3% milk in PBS and then incubating for 2 h at 37 °C. After washing the plate with PBS + 0.05% Tween 20 and then only PBS, as previously described, each well was incubated with LPS−biotin (Aurogene srl, Roma, Italy) diluted in 0.3% PBS-BSA at a working concentration of 5 μg/mL. The negative control contained only 0.3% PBS-BSA. The plate was incubated in the dark at 30 °C for 30 min. After washing, 100 μL/well of streptavidin−POD (Sigma-Aldrich, St. Louis, MO, USA) diluted at a ratio of 1:500 in 0.3% PBS-milk was added, followed by incubation in the dark for

https://doi.org/10.1021/acs.jmedchem.4c00810
J. Med. Chem. 2024, 67, 16145−16156

30 min at 30 °C. After another washing cycle, 150 μL/well of substrate solution composed of phosphocitrate buffer, TMB, DMSO, glycerol, and H_2O_2 was added, followed by incubation for 5 min. The reaction was stopped with 50 μL/well of 1 M HCl and the plate was read at 450 and 650 nm with a microplate spectrophotometer (Multiskan, Thermo Scientific, Waltham, MA, USA).

Antibiofilm Activity. Biofilm inhibition and eradication activities of the peptides were evaluated using two parameters: BPC and MBIC. For BPC, 100 μL of each peptide was added to the wells of a 96-well plate with peg lids in triplicate with 2-fold serial dilution of each peptide. Overnight cultures of *E. coli* TG1 and *K. pneumoniae* 43816 were diluted at a ratio of 1:100 and bacteria were grown until reaching an OD of 0.8 in 2xTy and LB, respectively. This bacterial suspension was diluted at a ratio of 1:1000, and 100 μL was added to the wells. Untreated bacteria were used as positive controls. The plate was incubated for 24 h at 37 °C and 110 rpm. Following incubation with peptides, the pegs were rinsed with sterile PBS and placed in a fresh 96-well F-bottom plate containing 180 μL of bacterial broth.

Bacteria were removed from the pegs by centrifuging for 20 min at 1400 rpm. The plate was incubated for 4 h at 37 °C and read at 595 nm. The BPC is the lowest concentration of an antibiotic that results in an OD595 nm difference of 80% in the mean of two control well readings.

For MBIC, 200 μL of bacterial suspension, obtained as above, was added to the wells of a 96-well plate with peg lids and incubated for 24 h at 37 °C and 110 rpm. Following incubation, 200 μL of each peptide diluted in bacterial broth was added to a fresh 96-well F-bottom plate in 2-fold serial dilutions of each peptide. The pegs were rinsed once with sterile PBS and placed in a plate containing the peptides. Untreated bacteria were used as positive controls. The plate was incubated for 24 h at 37 °C and 110 rpm. Following incubation with peptides, the pegs were rinsed with sterile PBS and placed in a fresh 96-well F-bottom plate containing 180 μL of bacterial broth. The bacteria were removed from the pegs by centrifuging for 20 min at 1400 rpm. The plate was incubated for 4 h at 37 °C and then read at 595 nm. The MBIC is the lowest concentration of an antibiotic that results in an OD595 nm difference of 80% of the mean of the two control well readings.

Skin Infection Model. BALB/C female mice were purchased from Charles River Laboratories Italia. They were 7 weeks old and weighed about 25 ± 3 g at the time of the experiments. The animals were maintained and handled in accordance with the Guidelines for Accommodation and Care of Animals (European Convention for the Protection of Vertebrate Animals Used for Experimental and Other Scientific Purposes) and internal guidelines. They underwent a four-day acclimation period after purchase. *E. coli*-luxCDABE was grown to an OD600 of 0.8 and resuspended in sterile PBS. All mice were infected with 1×10^8 CFU of *E. coli*-luxCDABE in 50 μL of PBS injected into the right side of the shaved dorsum.[35] Infected animals were divided randomly into two groups: the control and treated. The control group only received saline (50 μL); the other group was injected with 0.4 mg of BAMP2 (16 mg/kg) in 50 μL of sterile saline into the subcutaneous space of the infected area, 2 h after infection and every 24 h, three times. After each treatment, images of the luminescent bacteria were recorded in the anesthetized mice with an IVIS Lumina X5 (PerkinElmer) to monitor the infection. On the fourth day, the animals were euthanized with CO_2 after being anesthetized with isoflurane.

Skin cryosections were fixed in 4% PFA in PBS for 10 min at 2−8 °C and then rehydrated with PBS for 10 min. After that, the sections were incubated with 1% horse serum in PBS for 30 min at room temperature to block unspecific sites. After a wash with PBS, the skin sections were incubated with antimouse Ly6-G/Ly6-C conjugated with Alexa Fluor 488 (BioLegend) in 1% BSA overnight at 2−8 °C. The following day, the sections were washed three times with PBS and mounted on glass coverslips with ProLong Gold antifade reagent and DAPI (Molecular Probes). Samples were analyzed by a confocal laser microscope (Leica TCS SP5) at 364 λ_{ex} and 458 λ_{em} for a ProLong Diamond antifade mountant with DAPI and at 501 λ_{ex} and 523 λ_{em} for Atto 488. Images were analyzed with ImageJ, splitting the color into two channels and using the blue signal (DAPI) to evaluate the total number of cells in the tissue slice and the green signal (Ly6-G/Ly6-C-488) to obtain the number of monocytes as a ratio of the total cell number.

■ ASSOCIATED CONTENT

Supporting Information

The Supporting Information is available free of charge at https://pubs.acs.org/doi/10.1021/acs.jmedchem.4c00810.

HPLC chromatograms and MS spectra of BAMPs (S1); minimum inhibitory concentrations of monomers (S2); stability to serum proteolysis (S3 and S4); and mass spectra of the proteolytic fragments (S5) (PDF)

■ AUTHOR INFORMATION

Corresponding Author

Chiara Falciani − *Department of Medical Biotechnology, University of Siena, 53100 Siena, Italy;* orcid.org/0000-0002-1027-8482; Email: chiara.falciani@unisi.it

Authors

Giada Meogrossi − *Department of Medical Biotechnology, University of Siena, 53100 Siena, Italy*

Eva Tollapi − *Department of Medical Biotechnology, University of Siena, 53100 Siena, Italy;* orcid.org/0000-0001-6144-1078

Alessandro Rencinai − *Department of Medical Biotechnology, University of Siena, 53100 Siena, Italy;* orcid.org/0000-0002-3278-2778

Jlenia Brunetti − *Department of Medical Biotechnology, University of Siena, 53100 Siena, Italy;* orcid.org/0000-0001-8144-7186

Silvia Scali − *Department of Medical Biotechnology, University of Siena, 53100 Siena, Italy*

Eugenio Paccagnini − *Department of Life Sciences, University of Siena, 53100 Siena, Italy*

Mariangela Gentile − *Department of Life Sciences, University of Siena, 53100 Siena, Italy;* orcid.org/0000-0002-4928-4652

Pietro Lupetti − *Department of Life Sciences, University of Siena, 53100 Siena, Italy*

Simona Pollini − *Department of Experimental and Clinical Medicine, University of Florence, 50134 Florence, Italy; Microbiology and Virology Unit, Careggi University Hospital, 50134 Florence, Italy*

Gian Maria Rossolini − *Department of Experimental and Clinical Medicine, University of Florence, 50134 Florence, Italy; Microbiology and Virology Unit, Careggi University Hospital, 50134 Florence, Italy*

Andrea Bernini − *Department of Biotechnology, Chemistry and Pharmacy, University of Siena, 53100 Siena, Italy;* orcid.org/0000-0002-7528-2749

Alessandro Pini − *Department of Medical Biotechnology, University of Siena, 53100 Siena, Italy; Laboratory of Clinical Pathology, Santa Maria alle Scotte University Hospital, 53100 Siena, Italy; Setlance srl, 53100 Siena, Italy*

Luisa Bracci − *Department of Medical Biotechnology, University of Siena, 53100 Siena, Italy; Laboratory of Clinical Pathology, Santa Maria alle Scotte University Hospital, 53100 Siena, Italy;* orcid.org/0000-0002-0738-5746

Complete contact information is available at:

https://pubs.acs.org/10.1021/acs.jmedchem.4c00810

Author Contributions

G.M. and E.T. contributed equally to this work. C.F.: Conceptualization; S.S., E.P., M.G., P.L., S.P., G.M.R., A.B.: methodology; C.F., J.B., G.M., E.T., A.R.: investigation; C.F., A.P., L.B.: supervision; C.F.: writing—original draft; C.F., E.T., G.M., A.B.: writing—review and editing.

Funding

This work was funded by the EU within the NextGeneration EU-MUR PNRR Tuscany Health Ecosystem (Project no. ECS00000017-THE).

Notes

The authors declare no competing financial interest.

■ ACKNOWLEDGMENTS

We are grateful to Harry Mobley and his lab for the pGEN-luxCDABE plasmid. We thank Stefano Bindi for his contribution to animal care. We thank Prof. Francesco Luzzaro for providing the *E. coli* LC711/14 strain.

■ ABBREVIATIONS

α-CBH, α-chain of bovine hemoglobin; AMP, antimicrobial peptide; AMR, antimicrobial resistance; BAMP, branched antimicrobial peptide; BPC, biofilm prevention concentration; ELISA, enzyme-linked immunosorbent assay; Fmoc, fluorenylmethoxycarbonyl; KDO, 3-deoxy-α-D-manno-octulosonic acid; LPS, lipopolysaccharide; LTA, lipoteichoic acid; MDR, multidrug-resistant; MBIC, minimal biofilm inhibition concentration; MIC, minimum inhibitory concentration; SEM, scanning electron microscopy; streptavidin−POD, streptavidin−peroxidase; TEM, transmission electron microscopy; WHO, World Health Organization.

■ REFERENCES

(1) https://www.who.int/health-topics/antimicrobial-resistance, accessed on the 02/01/2024.
(2) Diamond, G.; Beckloff, N.; Weinberg, A.; Kisich, K. O. The roles of antimicrobial peptides in innate host defense. *Curr. Pharm. Des.* **2009**, *15* (21), 2377−2392.
(3) Uddin, S. J.; Shilpi, J. A.; Nahar, L.; Sarker, S. D.; Göransson, U. Editorial: Natural Antimicrobial Peptides: Hope for New Antibiotic Lead Molecules. *Front Pharmacol.* **2021**, *12*, No. 640938.
(4) Silva, O. N.; Torres, M. D. T.; Cao, J.; Alves, E. S. F.; Rodrigues, L. V.; Resende, J. M.; et al. Repurposing a peptide toxin from wasp venom into antiinfectives with dual antimicrobial and immunomodulatory properties. *Proc. Natl. Acad. Sci. U. S. A.* **2020**, *117* (43), 26936−26945.
(5) Wang, S.; Zeng, X.; Yang, Q.; Qiao, S. Antimicrobial Peptides as Potential Alternatives to Antibiotics in Food Animal Industry. *Int. J. Mol. Sci.* **2016**, *17* (5), 603.
(6) Cresti, L.; Falciani, C.; Cappello, G.; Brunetti, J.; Vailati, S.; Melloni, E.; et al. Safety evaluations of a synthetic antimicrobial peptide administered intravenously in rats and dogs. *Sci. Rep.* **2022**, *12* (1), 19294.
(7) Marianantoni, G.; Meogrossi, G.; Tollapi, E.; Rencinai, A.; Brunetti, J.; Marruganti, C.; et al. Antimicrobial Peptides Active in In Vitro Models of Endodontic Bacterial Infections Modulate Inflammation in Human Cardiac Fibroblasts. *Pharmaceutics.* **2022**, *14* (10), 2081.
(8) Brunetti, J.; Carnicelli, V.; Ponzi, A.; Di Giulio, A.; Lizzi, A. R.; Cristiano, L.; et al. Antibacterial and Anti-Inflammatory Activity of an Antimicrobial Peptide Synthesized with D Amino Acids. *Antibiotics (Basel).* **2020**, *9* (12), 840.
(9) Ritter, D.; Knebel, J.; Niehof, M.; Loinaz, I.; Marradi, M.; Gracia, R.; et al. In vitro inhalation cytotoxicity testing of therapeutic nanosystems for pulmonary infection. *Toxicol In Vitro.* **2020**, *63*, No. 104714.
(10) van der Weide, H.; Vermeulen-de Jongh, D. M. C.; van der Meijden, A.; Boers, S. A.; Kreft, D.; Ten Kate, M. T.; et al. Antimicrobial activity of two novel antimicrobial peptides AA139 and SET-M33 against clinically and genotypically diverse *Klebsiella pneumoniae* isolates with differing antibiotic resistance profiles. *Int. J. Antimicrob Agents.* **2019**, *54* (2), 159−166.
(11) van der Weide, H.; Brunetti, J.; Pini, A.; Bracci, L.; Ambrosini, C.; Lupetti, P.; Paccagnini, E.; et al. Investigations into the killing activity of an antimicrobial peptide active against extensively antibiotic-resistant K. *pneumoniae and P. aeruginosa. Biochim Biophys Acta Biomembr.* **2017**, *1859* (10), 1796−1804.
(12) Ying, Y.; Wang, H.; Xi, X.; Ma, C.; Liu, Y.; Zhou, M.; et al. Design of N-Terminal Derivatives from a Novel Dermaseptin Exhibiting Broad-Spectrum Antimicrobial Activity against Isolates from Cystic Fibrosis Patients. *Biomolecules.* **2019**, *9* (11), 646.
(13) Gou, S.; Li, B.; Ouyang, X.; Ba, Z.; Zhong, C.; Ni, J. Tuning the Activity of Anoplin by Dendrimerization of Lysine and Lipidation of the N-Terminal. *ACS Omega.* **2021**, *6* (33), 21359−21367.
(14) Wojciechowska, M.; Macyszyn, J.; Miszkiewicz, J.; Grzela, R.; Trylska, J. Stapled Anoplin as an Antibacterial Agent. *Front Microbiol.* **2021**, *12*, No. 772038.
(15) Zhang, G. W.; Lai, S. J.; Yoshimura, Y.; Isobe, N. Expression of cathelicidins mRNA in the goat mammary gland and effect of the intramammary infusion of lipopolysaccharide on milk cathelicidin-2 concentration. *Vet. Microbiol.* **2014**, *170* (1−2), 125−134.
(16) Bracci, L.; Falciani, C.; Lelli, B.; et al. Synthetic peptides in the form of dendrimers become resistant to protease activity. *J. Biol. Chem.* **2003**, *278* (47), 46590−46595.
(17) Falciani, C.; Lozzi, L.; Pollini, S.; Luca, V.; Carnicelli, V.; Brunetti, J.; et al. Isomerization of an antimicrobial peptide broadens antimicrobial spectrum to gram-positive bacterial pathogens. *PLoS One.* **2012**, *7* (10), No. e46259.
(18) Falciani, C.; Lozzi, L.; Pini, A.; Corti, F.; Fabbrini, M.; Bernini, A.; et al. Molecular basis of branched peptides resistance to enzyme proteolysis. *Chem. Biol. Drug Des.* **2007**, *69* (3), 216−221.
(19) Brunetti, J.; Roscia, G.; Lampronti, I.; Gambari, R.; Quercini, L.; Falciani, C.; Bracci, L.; Pini, A. Immunomodulatory and Anti-inflammatory Activity in Vitro and in Vivo of a Novel Antimicrobial Candidate. *J. Biol. Chem.* **2016**, *291* (49), 25742−25748.
(20) Serna, N.; López-Laguna, H.; Aceituno, P.; Rojas-Peña, M.; Parladé, E.; Voltà-Durán, E.; Martínez-Torró, C.; Sánchez, J. M.; Di Somma, A.; Carratalá, J. V.; Livieri, A. L.; Ferrer-Miralles, N.; Vázquez, E.; Unzueta, U.; Roher, N.; Villaverde, A. Efficient Delivery of Antimicrobial Peptides in an Innovative, Slow-Release Pharmacological Formulation. *Pharmaceutics* **2023**, *15* (11), 2632.
(21) Quercini, L.; Brunetti, J.; Riolo, G.; Bindi, S.; Scali, S.; Lampronti, I.; D'Aversa, E.; Wronski, S.; Pollini, S.; Gentile, M.; Lupetti, P.; Rossolini, G. M.; Falciani, C.; Bracci, L.; Pini, A. An antimicrobial molecule mitigates signs of sepsis in vivo and eradicates infections from lung tissue. *FASEB J.* **2020**, *34* (1), 192−207.
(22) Timmons, P. B.; Hewage, C. M APPTEST is a novel protocol for the automatic prediction of peptide tertiary structures. *Briefings Bioinf.* **2021**, *22* (6), No. bbab308.
(23) Nordström, R.; Nyström, L.; Andrén, O. C. J.; Malkoch, M.; Umerska, A.; Davoudi, M.; et al. Membrane interactions of microgels as carriers of antimicrobial peptides. *J. Colloid Interface Sci.* **2018**, *513*, 141−150.
(24) Ciumac, D.; Gong, H.; Hu, X.; Lu, J. R. Membrane targeting cationic antimicrobial peptides. *J. Colloid Interface Sci.* **2019**, *537*, 163−185.
(25) Epand, R. M.; Vogel, H. J. Diversity of antimicrobial peptides and their mechanisms of action. *Biochim. Biophys. Acta* **1999**, *1462* (1−2), 11−28.
(26) Boix-Lemonche, G.; Lekka, M.; Skerlavaj, B. A Rapid Fluorescence-Based Microplate Assay to Investigate the Interaction

of Membrane Active Antimicrobial Peptides with Whole Gram-Positive Bacteria. *Antibiotics (Basel)*. **2020**, *9* (2), 92.
(27) Benfield, A. H.; Henriques, S. T. Mode-of-Action of Antimicrobial Peptides: Membrane Disruption vs. *Intracellular Mechanisms. Front Med. Technol.* **2020**, *2*, No. 610997.
(28) Moretta, A.; Scieuzo, C.; Petrone, A. M.; Salvia, R.; Manniello, M. D.; Franco, A.; et al. Antimicrobial Peptides: A New Hope in Biomedical and Pharmaceutical Fields. *Front Cell Infect Microbiol.* **2021**, *11*, No. 668632.
(29) Roy, R.; Tiwari, M.; Donelli, G.; Tiwari, V. Strategies for combating bacterial biofilms: A focus on anti-biofilm agents and their mechanisms of action. *Virulence.* **2018**, *9* (1), 522−554.
(30) Macià, M. D.; Rojo-Molinero, E.; Oliver, A. Antimicrobial susceptibility testing in biofilm-growing bacteria. *Clin Microbiol Infect.* **2014**, *20* (10), 981−990.
(31) Lane, M. C.; Alteri, C. J.; Smith, S. N.; Mobley, H. L. Expression of flagella is coincident with uropathogenic *Escherichia coli* ascension to the upper urinary tract. *Proc. Natl. Acad. Sci. U. S. A.* **2007**, *104* (42), 16669−16674.
(32) Li, H.; Niu, J.; Wang, X.; Niu, M.; Liao, C. The Contribution of Antimicrobial Peptides to Immune Cell Function: A Review of Recent Advances. *Pharmaceutics.* **2023**, *15* (9), 2278.
(33) Brandt, S. L.; Klopfenstein, N.; Wang, S.; Winfree, S.; McCarthy, B. P.; Territo, P. R.; et al. Macrophage-derived LTB4 promotes abscess formation and clearance of Staphylococcus aureus skin infection in mice. *PLoS Pathog.* **2018**, *14* (8), No. e1007244.
(34) Jo, S.; Kim, T.; Iyer, V. G.; Im, W. CHARMM-GUI: a web-based graphical user interface for CHARMM. *J. Comput. Chem.* **2008**, *29* (11), 1859−1865. PMID: 18351591.
(35) Pletzer, D.; Mansour, S. C.; Hancock, R. E. W. Synergy between conventional antibiotics and anti-biofilm peptides in a murine, sub-cutaneous abscess model caused by recalcitrant ESKAPE pathogens. *PLoS Pathog.* **2018**, *14* (6), No. e1007084.

https://doi.org/10.1021/acs.jmedchem.4c00810
J. Med. Chem. 2024, 67, 16145−16156